Chemical footprinting and kinetic assays reveal dual functions for highly conserved eukaryotic tRNA^{His} guanylyltransferase residues

Received for publication, February 18, 2019, and in revised form, April 16, 2019 Published, Papers in Press, April 18, 2019, DOI 10.1074/jbc.RA119.007939

Ashanti O. Matlock, Brian A. Smith[1], and Jane E. Jackman[2]

From the Department of Chemistry and Biochemistry, Center for RNA Biology, and Ohio State Biochemistry Program, The Ohio State University, Columbus, Ohio 43210

Edited by Ronald C. Wek

tRNA^{His} guanylyltransferase (Thg1) adds a single guanine to the −1 position of tRNA^{His} as part of its maturation. This seemingly modest addition of one nucleotide to tRNA^{His} ensures translational fidelity by providing a critical identity element for the histidyl aminoacyl tRNA synthetase (HisRS). Like HisRS, Thg1 utilizes the GUG anticodon for selective tRNA^{His} recognition, and Thg1-tRNA complex structures have revealed conserved residues that interact with anticodon nucleotides. Separately, kinetic analysis of alanine variants has demonstrated that many of these same residues are required for catalytic activity. A model in which loss of activity with the variants was attributed directly to loss of the critical anticodon interaction has been proposed to explain the combined biochemical and structural results. Here we used RNA chemical footprinting and binding assays to test this model and further probe the molecular basis for the requirement for two critical tRNA-interacting residues, His-152 and Lys-187, in the context of human Thg1 (hThg1). Surprisingly, we found that His-152 and Lys-187 alanine-substituted variants maintain a similar overall interaction with the anticodon region, arguing against the sufficiency of this interaction for driving catalysis. Instead, conservative mutagenesis revealed a new direct function for these residues in recognition of a non–Watson–Crick G_{-1}:A_{73} bp, which had not been described previously . These results have important implications for the evolution of eukaryotic Thg1 from a family of ancestral promiscuous RNA repair enzymes to the highly selective enzymes needed for their essential function in tRNA^{His} maturation.

tRNAs are nearly all transcribed as precursor-tRNA with additional 5′ and 3′ sequences. These excess sequences are subsequently removed by endonucleases and/or exonucleases to produce mature tRNA with uniform 5′- and 3′-ends for their use in translation (1). However, in the case of histidine tRNA (tRNA^{His}),[3] the presence of an additional 5′ guanosine nucleotide (G_{-1}) distinguishes it from all other tRNAs and is a critical identity element for efficient aminoacylation by histidyl-tRNA synthetase (HisRS) (2–5). The HisRS requirement for G_{-1} is a conserved feature throughout all domains of life, and a relatively small number of species described so far deviate from this rule (6–9).

Interestingly, bacteria and eukaryotes have evolved different mechanisms of incorporating the additional −1 nucleotide into tRNA^{His} (10–15). In almost all bacteria and some eukaryotic organelles, the G_{-1} nucleotide is encoded in the tRNA^{His} gene, incorporated by transcription, and retained in the mature tRNA through aberrant cleavage by 5′-endonuclease RNase P (11, 12, 15). In contrast, most eukaryotes studied to date incorporate G_{-1} posttranscriptionally to the processed 5′ end of tRNA^{His} (10, 16). This posttranscriptional addition of G_{-1} is performed by the tRNA^{His} guanylyltransferase (Thg1), which was first described in *Saccharomyces cerevisiae* and produces a non–Watson–Crick (non-WC) G_{-1}:A_{73} bp as a result of this reaction (Fig. 1*A*) (16).

Shortly after the gene encoding Thg1 in *S. cerevisiae* was identified, it was demonstrated that this enzyme also performed Watson–Crick–templated 3′ to 5′ polymerase activity, in addition to the non-WC– dependent activity described initially (17). Despite a lack of overall sequence identity to 5′ to 3′ polymerases, the crystal structure of human Thg1 (hThg1) revealed that the active sites of 3′ to 5′ and 5′ to 3′ polymerases were structurally analogous and both enzymes share a common two metal ion–mediated mechanism (18, 19).

Catalysis of G_{-1} addition to tRNA^{His} by Thg1 occurs in three chemical steps (Fig. 1*B*) (19–21). First, 5′ monophosphorylated tRNA^{His}, the product of RNase P cleavage, is activated via adenylylation using ATP. Next, the adenylylated intermediate is attacked by the 3′-hydroxyl of the incoming GTP, completing the nucleotidyl transfer step. Finally, pyrophosphate is released, returning the 5′-end to its original monophosphorylated status, and extended by one nucleotide (16, 20). Kinetic and structural studies have revealed important roles for highly conserved Thg1 residues in catalyzing these chemical steps both *in vitro*

This work was supported by National Institutes of Health Grant R01 GM087543 (to J. E. J.), a Cellular and Molecular Biosciences training grant (to A. O. M.), and a Center for RNA Biology fellowship (to B. A. S.). The authors declare that they have no conflicts of interest with the contents of this article. The content is solely the responsibility of the authors and does not necessarily represent the official views of the National Institutes of Health.

This article contains Figs. S1–S4.

[1] Present address: Dept. of Natural Sciences, Lawrence Technical University, E-mail: bsmith2@ltu.edu.

[2] To whom correspondence should be addressed. Tel.: 614-247-8097; E-mail: jackman.14@osu.edu.

[3] The abbreviations used are: tRNA^{His}, histidine tRNA; HisRS, histidyl aminoacyl tRNA synthetase; WC, Watson–Crick; CMCT, 1-cyclohexyl-(2-morpholinoethyl)carbodiimide metho-*p*-toluenesulfonate.

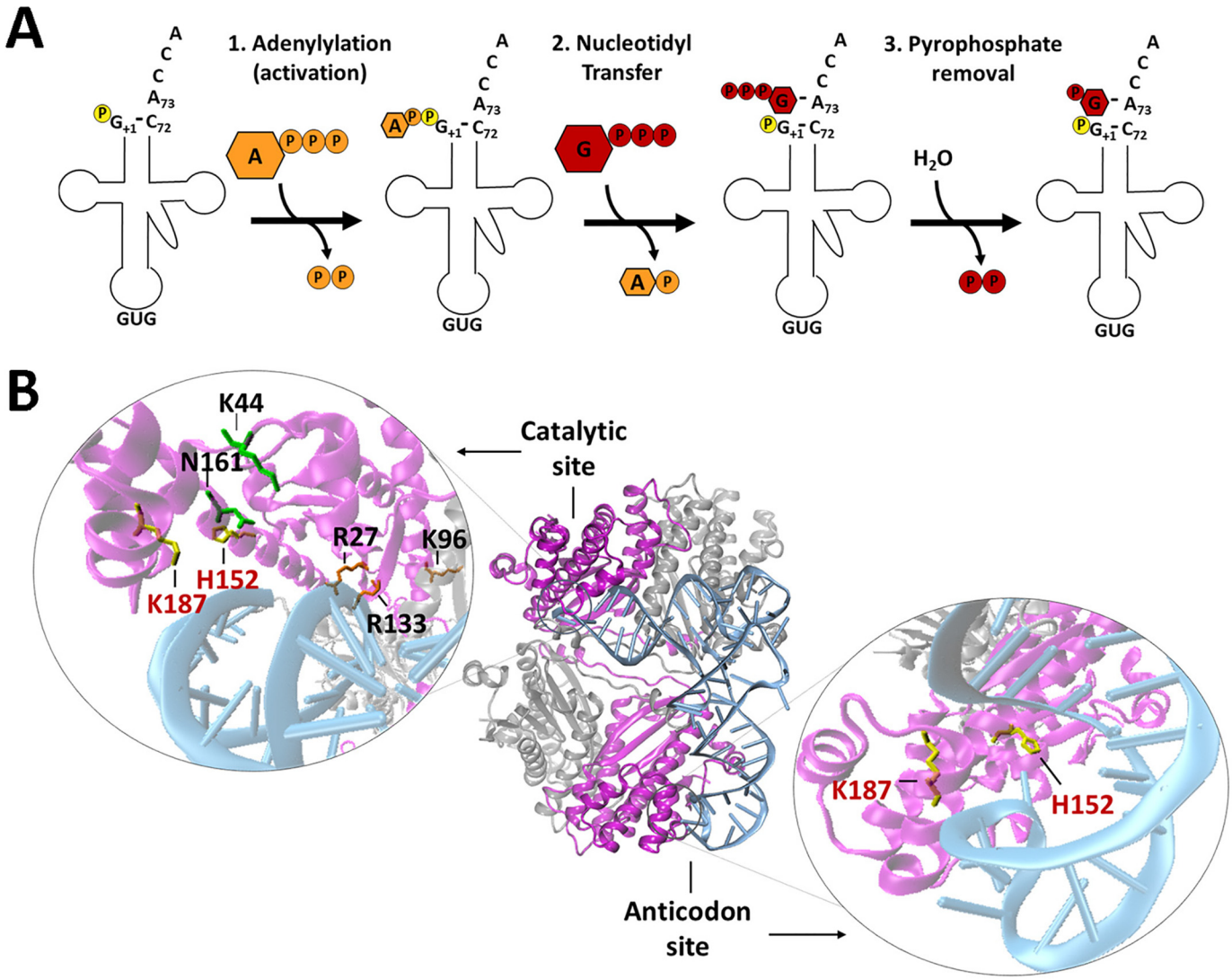

Figure 1. Thg1 enzymes catalyze G_{-1} addition to $tRNA^{His}$. *A*, overall reaction catalyzed by Thg1. 5′-monophosphorylated tRNA is first activated by transfer of AMP (*orange*) to the 5′-phosphate (*yellow*) from ATP. The incoming GTP nucleotide (*red*) attacks the activated 5′-phosphate generating the G_{-1}-containing $tRNA^{His}$. The additional phosphates on the G_{-1} product are removed by a pyrophosphate removal step that is catalyzed by the same two-metal ion active site, generating 5′-monophosphorylated G_{-1}-containing $tRNA^{His}$. *B*, *Candida albicans* $tRNA^{His}$ guanylyltransferase bound to $tRNA^{His}$ lacking the G_{-1} nucleotide. This depiction of the CaThg1-tRNA complex was created using PDB ID 3WC1. CaThg1 is a homotetramer that binds two tRNA substrates. For clarity, one of two bound tRNAs is shown (*blue*) and monomers interacting with the tRNA at the 5′-end and at the anticodon loop are highlighted in *purple*. Absolutely conserved Thg1 residues from 15 representative eukaryotic organisms including *C. albicans* include Lys-44, Asn-161, Arg-27, Lys-95, Arg-130, His-152, and Lys-187 (human Thg1 numbering). Side chains are colored according to their known functions (*top left image*), with *green* indicating roles in adenylylation, *orange* indicating function in nucleotidyl transfer, and with the His-152 and Lys-187 residues that are the focus of this work highlighted in *yellow*. His-152 and Lys-187 also appear in proximity to the anticodon stem loop, where a direct interaction between His-152 and tRNA anticodon nucleotides had been previously observed (*bottom-right image*).

and *in vivo* (18, 19, 22–27). These include residues that specifically facilitate adenylylation (Lys-44 and Asn-161 according to hThg1 numbering), and residues that selectively facilitate nucleotidyl transfer (Arg-27, Lys-95, and Arg-130) (Fig. 1) (19, 22, 25). These important catalytic roles are underscored by the very high (at or near 100%) conservation of these residues among representative eukaryotic Thg1 enzymes studied to date (22). However, these biochemical studies also identified several catalytically essential residues that were similarly conserved, suggesting important roles, but for which specific functions in catalysis remained unknown. Residues His-152 and Lys-187 (hThg1 numbering) were among the most defective of these previously studied alanine variants, exhibiting no detectable ability to add G_{-1} to $tRNA^{His}$ *in vitro* or *in vivo* (18, 22).

Reflecting the important role of G_{-1} in specifying $tRNA^{His}$ identity, eukaryotic Thg1 enzymes are strictly specific for $tRNA^{His}$, and this specificity is accomplished by recognition of the $tRNA^{His}$ GUG anticodon (28). A crystal structure of *Candida albicans* Thg1 (CaThg1) bound to $tRNA^{His}$ revealed a network of molecular interactions between the enzyme and the anticodon loop, consistent with the role of the anticodon nucleotides as the major identity element for eukaryotic Thg1. Interestingly, His-152 was featured in this network of Thg1 residues that directly interact with the anticodon, and residue Lys-187 was also located nearby (Fig. 1*B*) (23, 28). Thus, a model was proposed based on the location of these residues near the critical anticodon element. This model attributed the absence of G_{-1} addition activity with the alanine variants to disruption of

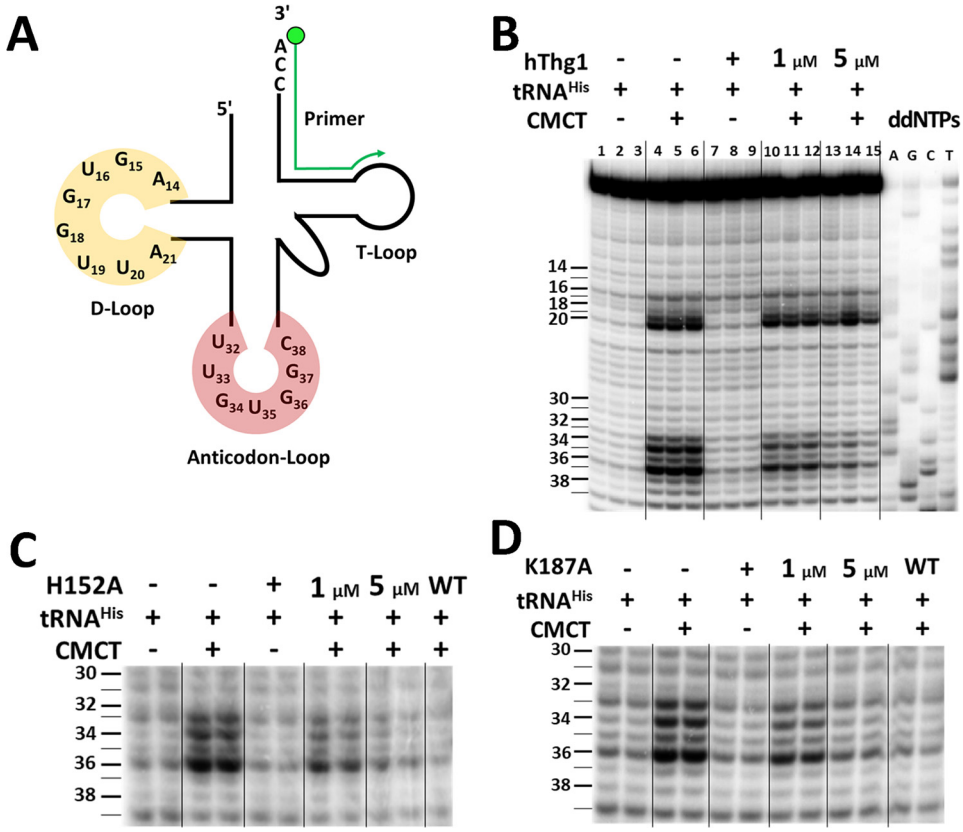

Figure 2. Chemical footprinting of tRNA^{His} by CMCT. *A*, illustration of possible nucleobases susceptible to CMCT modification and the annealing location of a 5′-end–labeled primer used to extend the modified tRNA. CMCT modifies the N-1 and N-3 positions of guanine and uracil, respectively. Modified sites in the anticodon loop and D-loop result in a block to primer extension. *B*, CMCT footprinting was performed with 50 nM of unlabeled *in vitro* transcribed tRNA^{His}, and the indicated concentrations of WT hThg1. Numbering to the left of the primer extension results corresponds to site of primer extension stop for selected nucleotides from D-loop and anticodon loop. Each set of three lanes corresponds to independent reactions performed in triplicate and analyzed separately. Quantification of these data are presented in Fig. S1. *C* and *D*, CMCT footprinting with hThg1 H152A and K187A variants at 1 and 5 μM and 50 nM of unlabeled *in vitro* transcribed tRNA^{His} was performed in duplicate. The hThg1 WT control reaction contained 5 μM of enzyme and 50 nM of unlabeled *in vitro* transcribed tRNA^{His}. Only nucleotides of the anticodon loop showing significant protection from CMCT modification are shown for clarity.

the enzyme's interaction with the anticodon leading to an inability to correctly position the tRNA 5′-end in the active site (23). However, this hypothesis was not directly tested in any mechanistic assays.

We sought to further investigate the molecular basis for the inactivity of alanine variants of His-152 and Lys-187 using chemical footprinting and kinetic assays. Here, we show that removal of either of these residues does not significantly diminish chemical protection of the anticodon nucleotides by the variant enzymes. Moreover, instead of being catalytically inactive as previously thought, we discovered that the H152A and K187A hThg1 variants exhibit robust 3′ to 5′ addition activity with tRNA variant substrates that have not been tested previously, but which allow WC-dependent nucleotide addition. Finally, we demonstrated that the inability of the alanine variants to catalyze the non-WC reaction to create the G_{-1}:A_{73} bp results primarily from a defect in adenylylation, the first step of the 3′ to 5′ addition reaction (Fig. 1*B*). Together, these results suggest dual independent roles for His-152 and Lys-187 residues in the context of Thg1 catalysis and tRNA recognition and indicate that Thg1 utilizes independent WC and non-WC bp recognition sites involving distinct sets of residues.

Results

hThg1 variants and their interaction with the tRNA^{His} anticodon

To probe the interaction of hThg1 with tRNA^{His} at single nucleotide resolution, we performed chemical footprinting with 1-cyclohexyl-(2-morpholinoethyl)carbodiimide metho-*p*-toluene sulfonate (CMCT). CMCT was chosen because of its ability to modify the N-1 and N-3 positions of unpaired guanine and uracil residues, respectively, and G/U nucleotides make up six of the seven nucleotides within the tRNA^{His} anticodon loop. Positions of CMCT modification were identified as blocks to primer extension using a primer complementary to the 3′-end of the tRNA (Fig. 2*A*). Consistent with the expected tRNA structure, CMCT-dependent modification of the *in vitro* transcribed tRNA^{His} was readily detected in the anticodon and D-loops of the tRNA in the absence of protein (Fig. 2*B*, compare *lanes 1–3 versus 4–6*). The location of the primer at the 3′-end prevented visualization of T-loop nucleotides.

Modification by CMCT was then performed on the same tRNA^{His} substrate in the presence of 1 μM and 5 μM hThg1 (concentrations chosen according to the ~1 μM $K_{D,app,tRNA}$ measured previously using kinetic assays) (19). Protection from CMCT modification across the entire anticodon loop was

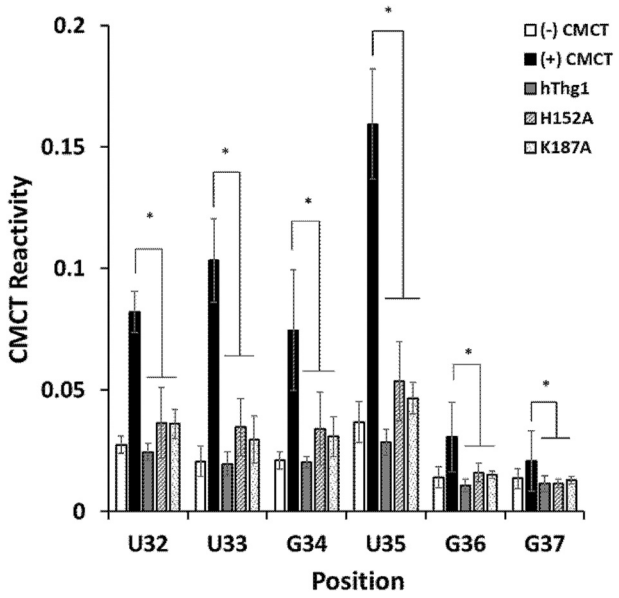

Figure 3. Quantification of normalized CMCT reactivity for WT and variant hThg1 enzymes. Reactivity with CMCT at each indicated position in the $tRNA^{His}$ anticodon loop was quantified based on the intensity of the band corresponding to each primer extension product normalized to the band intensity observed for the full-length tRNA in the same reactions (see Fig. 2). Data represent the average reactivity from three experiments, with *error bars* corresponding to the S.E. of each measurement. Statistical tests for significance were measured using a two-tailed *t* test comparing the protein-treated samples (hThg1 = *gray*; H152A = *striped*; K187A = *dotted*) with the CMCT-only control (no protein; *black*). All protein-treated samples exhibited differences from the CMCT-only control reactivity with p values < 0.05 (denoted by a single asterisk *).

observed with WT hThg1 in a concentration-dependent manner, consistent with previous structural and biochemical data suggesting the interaction between Thg1 and this part of the tRNA (Fig. 2*B*, *lanes 10–15*; Fig. S1).

We then used this assay to test the role of His-152 and Lys-187 in maintaining the anticodon interaction that was previously hypothesized to be responsible for orienting the tRNA 5′-end in the active site for catalysis. Interestingly, both H152A and K187A variant enzymes display very similar patterns of CMCT protection to WT hThg1 (Fig. 2, *C* and *D*), with quantification also revealing statistically significant protection of anticodon nucleotides compared with the no Thg1 controls (Fig. 3). Moreover, no statistically significant differences were identified between the levels of protection observed for either of the variants at each anticodon loop position compared with WT hThg1. Filter-binding assays were used to determine apparent affinity for $tRNA^{His}$ for each variant enzyme (Fig. S2; Table 1). The K187A variant exhibited a modest binding defect (about 5-fold) compared with WT consistent with this residue playing some role in overall tRNA binding, possibly through electrostatic interaction with the tRNA backbone. For H152A, the observed binding defect was more severe (~25-fold compared with WT) which was again consistent with the previously observed interaction of this residue with tRNA (Table 1). Nonetheless, the ability of the H152A variant to significantly protect the anticodon nucleotides from chemical modification suggests that sufficient binding occurs under the conditions of the assays performed here. Taken together, these data indicate that the severe catalytic defects associated with H152A and K187A variants cannot be attributed simply to a loss of the overall anticodon interaction that causes subsequent misplacement of the tRNA 5′-end in the active site. Instead, the loss of activity may be because of other, possibly more direct, roles of His-152 and Lys-187 in catalysis.

Unexpected Watson–Crick–dependent addition activities of His-152 and Lys-187 variants

Thg1 is a homotetramer that binds to two tRNA substrates. In the complex, the two tRNA molecules are bound asymmetrically, with the anticodon end of each tRNA in one monomer, and the 5′-end (site of G_{-1} addition) located in another monomer (Fig. 1*B*) (18, 23). Thus, the possibility of nonequivalent roles for residues derived from different monomers was considered. Indeed, His-152 and Lys-187 residues found in the two subunits that do not interact with the anticodon end of the tRNA are located relatively near the G_{-1} addition site, although the lack of interpretable electron density for tRNA nucleotides at the active site prevents observation of any direct contacts between these residues and the bound tRNA. Previous studies demonstrated that alteration of His-152 and Lys-187 to alanine causes complete loss of G_{-1} addition activity with WT $tRNA^{His}$, yet no available structural information helps to rationalize whether either of these residues plays a direct role in the chemistry of nucleotide addition, possibly in addition to its interaction with the bound tRNA.

For all previous studies testing the ability of hThg1 variants to catalyze G_{-1} addition, the WT $tRNA^{His}$ that contains an A_{73} discriminator nucleotide was used as the substrate in these assays (22, 23). However, an alternative substrate that contains a C_{73} discriminator nucleotide has also been utilized extensively in other studies, because of the ability of Thg1 enzymes to act as a "reverse polymerase" and incorporate multiple Watson–Crick base paired nucleotides into this substrate (17, 21, 29, 32). We sought to revisit the effects of alterations at His-152 and Lys-187 by testing the WC-dependent addition activity with the C_{73}-$tRNA^{His}$ substrate, which had not been tested previously. For these assays, 5′-end labeled substrate was incubated with varied concentrations of hThg1 enzyme in the presence of ATP and GTP. After quenching reactions with EDTA and RNase A (which cleaves at the site of the *red arrow* shown in Fig. 4), reactions were subsequently treated with phosphatase. The use of phosphatase exploits the difference in accessibility of the labeled 5′-phosphate in unreacted substrate *versus* in nucleotide addition products where the labeled phosphate is protected from phosphatase removal. Thus, labeled oligonucleotide fragments corresponding to reaction products can be resolved from labeled P_i by TLC (Fig. 4*A*) (28). As expected based on previous results, WT hThg1 produced products corresponding to addition of multiple G-nucleotides (G_{-1}pGpC and G_{-2}pG_{-1}pGpC) to C_{73}-$tRNA^{His}$ (Fig. 4*A*). Surprisingly, however, K187A catalyzed robust nucleotide addition to this substrate, and H152A was also active, although to a noticeably lesser extent (Fig. 4*A*). These results are in stark contrast to the complete lack of catalytic activity observed in at least three different studies for H152A and K187A variants with the WT $tRNA^{His}$ (18, 22, 23).

Table 1
Biochemical characterization of human Thg1 variants
ND, not determined.

	hThg1	H152A	H152F	K187A
k_{obs} ppp-tRNA^{His} (min^{-1})				
G_{-1}:A_{73} (non-WC)	0.0087 ± 0.001	0.00048 ± 0.0004[a]	0.0026 ± 0.0007[a]	0.0026 ± 0.0006[a]
G_{-1}:C_{73} (WC)	0.0036 ± 0.003	0.015 ± 0.005	0.011 ± 0.003	0.018 ± 0.004
$K_{D,tRNAHis}$ (nM)	200 ± 30	5040 ± 620[b]	ND	1060 ± 150

[a] Observed rate determined using the method of linear initial rates.
[b] $K_{D,app}$ derived from the fit represents an estimated value, because saturation of binding may not have been observed even at the highest concentration (12 μM) of enzyme achievable in the assays.

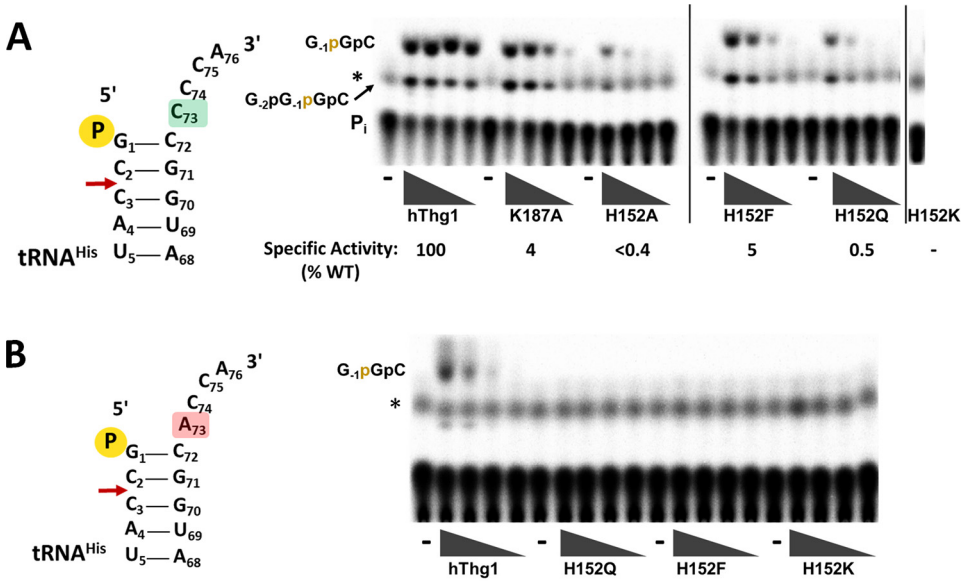

Figure 4. Watson–Crick *versus* non-Watson–Crick addition activities of hThg1 variants. *A*, WC-dependent G_{-1} addition across from a C_{73} discriminator nucleotide was measured by phosphatase protection assay. Reactions contained 5′-^{32}P–labeled C_{73}-tRNA^{His} and decreasing concentrations (36 μM-0.29 μM, in 5-fold serial dilutions) of hThg1 enzymes and incubated at room temperature for 2 h. The diagram to the *left* shows the aminoacyl-acceptor stem of the labeled tRNA^{His} substrate (the rest of the tRNA is omitted for clarity), with the labeled 5′-phosphate indicated in *yellow*, and the *red arrow* indicating cleavage site with RNase A to yield the G_{-1}pGpC product fragment that is visualized by TLC after G_{-1} addition. The presence of additional C_{74} and C_{75} nucleotides in the substrate 3′-end enables polymerization of additional WC-paired G-nucleotides to yield G_{-2}pG_{-1}pGpC product, as described previously (17, 18). Lanes indicated by (−) correspond to no enzyme control reactions. A labeled species (indicated by *) that occurs as a result of the labeling procedure but is not a product of enzyme reaction because it is present in equal amounts to the no enzyme control, is indicated. Quantification of specific activity exhibited by each enzyme was performed as in "Experimental Procedures," and percent specific activity relative to WT for each active enzyme is indicated below the panel. *B*, assays testing non-WC addition of G_{-1} to WT tRNA^{His} were performed as described in (*A*), but with the A_{73}-tRNA^{His} substrate, which was also processed as indicated by the diagram to the *left* of the panel to generate the indicated G_{-1}pGpC or P_i products (and the same nonenzyme-dependent species labeled with *), as indicated. The lack of observable activity prevents comparison of actual specific activity, but based on the inactivity of reactions containing the highest (36 μM) enzyme, it can be estimated that the variants are at least 10^4-fold defective relative to the WT.

Because the specific activity of the H152A variant was quantifiably weaker than that of K187A hThg1 (<0.4% of WT compared with 5% for K187A; Fig. 4*A*), we further probed the nature of the requirement for histidine at this position by making conservative alterations to either phenylalanine, glutamine, or lysine. These replacements for His-152 were chosen to mimic different biochemical properties (aromatic, hydrogen-bonding capacity, and possible positive charge, respectively) of the native histidine side chain. The H152K alteration did not exhibit any activity in any assay, with any tested substrate (Fig. 4*A* and data not shown) and was not pursued further. Interestingly, the H152F variant resulted in the most enhancement of WC-dependent G_{-1} addition activity compared with the original alanine alteration, whereas the H152Q alteration caused a modest but detectable increase in specific activity compared with H152A (Fig. 4*A*). Nonetheless, consistent with previous results for H152A hThg1 (18), none of these alternative His-152 replacements elicited any detectable non-WC addition of G_{-1} across from A_{73} with WT tRNA^{His} compared with the WT enzyme (Fig. 4*B*). Thus, we conclude that His-152 and Lys-187 play more important roles during the formation of a non-WC G_{-1}:A_{73} bp than for the WC G_{-1}:C_{73} nucleotide addition.

We considered two possible explanations for the different patterns of activity of the His-152 and Lys-187 variants with the C_{73}- *versus* A_{73}-containing tRNA. First, His-152 and/or Lys-187 may interact specifically with the discriminator A_{73}, and loss of direct contacts to the A_{73} nucleotide could be the cause of abrogated activity with A_{73}, but not C_{73}, variant tRNA. Alternatively, His-152 and/or Lys-187 could be involved in discriminating between the two types of bp (non-WC *versus* WC), and thus particularly required for efficiency of the non-WC interaction. We reasoned that testing the ability of each variant to perform U_{-1} addition with the WT (A_{73}) tRNA would allow us to distinguish between these possibilities, because this reaction would also measure a WC-dependent activity (formation of a U_{-1}:A_{73} bp), but the substrate would also retain an A_{73} nucle-

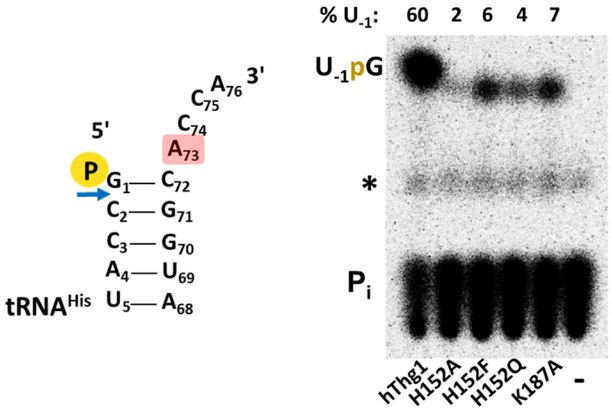

Figure 5. Thg1 variants perform Watson–Crick U_{-1} addition to A_{73}-tRNA^{His}. WC-dependent U_{-1} addition across from the A_{73} discriminator nucleotide was measured by phosphatase protection assay. Reactions contained 5′-^{32}P–labeled A_{73}-tRNA^{His} and 36 μM hThg1 enzymes and were incubated at room temperature for 2 h. The diagram to the *left* shows the aminoacyl-acceptor stem of the labeled tRNA^{His} substrate (the rest of the tRNA is omitted for clarity), with the labeled 5′-phosphate indicated in *yellow*, and the *blue arrow* indicating cleavage site with RNase T1 to yield the U_{-1}pG product fragment after U_{-1} addition, and P_i from remaining unreacted substrate. The identity of the labeled reaction products is indicated on the TLC image, including the nonenzyme-dependent species marked with an asterisk (*) that is also observed in the no enzyme control reactions.

otide in this case. Under identical experimental conditions used in experiments shown in Fig. 4*B*, we observed that each of the active His-152/Lys-187 variants for G_{-1}:C_{73} addition also performed readily detectable U_{-1} addition to the A_{73}-tRNA, albeit less efficiently than the WT hThg1 (Fig. 5). The H152F variant again exhibited slightly stronger activity than either A or Q alterations. Thus, the need for His-152 and Lys-187 residues for G_{-1}:A_{73} addition cannot be attributed solely to a requirement for these side chains to specifically interact with the discriminator A_{73} nucleotide, but rather to an interaction with the entire non-WC G_{-1}:A_{73} bp during catalysis.

His-152 and Lys-187 play critical roles in activation of tRNA^{His} for non-WC addition

To further define the role of His-152 and Lys-187 in the non-WC G_{-1} addition reaction, we took advantage of our previous kinetic framework that allowed us to separate the three chemical steps of the G_{-1} addition reaction to tRNA^{His} (Fig. 1*A*). We previously demonstrated that use of a 5′ triphosphorylated tRNA^{His} (ppp-tRNA^{His}) substrate bypasses the requirement for activation of the tRNA with ATP by providing an alternative activated 5′-phosphate at the tRNA 5′-end, thus enabling measurement of the rate-limiting step for nucleotidyl transfer (Fig. 1, step 2) (19, 28). In contrast to the complete lack of G_{-1} addition activity with any tested His-152 or Lys-187 variant with monophosphorylated A_{73}-tRNA^{His} (Fig. 4*B*), G_{-1} addition activity was readily observed for all of the variants with this same tRNA when presented in triphosphorylated form (ppp-tRNA^{His}). This is evident from the release of labeled pyrophosphate (which is also further hydrolyzed to P_i during the assay) with all tested enzymes (Fig. 6).

To quantify these effects, single turnover rate constants (k_{obs}) were compared for WC *versus* non-WC base-paired additions to triphosphorylated tRNAs (Table 1; Figs. S3 and S4). All assays were performed at high concentrations of enzyme (15 μM) and GTP (1 mM), which are saturating for this activity catalyzed by WT hThg1. Non-WC addition of G_{-1} to A_{73}-tRNA^{His} was significantly reduced for H152A by ~95% compared with WT. The stimulatory effect of the H152F variant was readily observed resulting in a 5-fold improvement in k_{obs} compared with the alanine variant (Table 1; Fig. S3). However, none of these effects are as severe as the $\geq 10^4$-fold loss of activity that was evident in the assays with the monophosphorylated p-tRNA^{His} (Fig. 4*B*) (18, 19). Therefore, we conclude that the requirement for His-152 and Lys-187 during addition of the non-WC G_{-1} nucleotide to A_{73}-tRNA^{His} primarily reflects an important role for these residues in the first (activation) step of the reaction. Moreover, and once the 5′-end activation step is completed, the need for His-152 and Lys-187 is no longer as critical (Fig. 1).

Interestingly, for the WC G:C reaction, k_{obs} were affected quite differently, with the variant enzymes exhibited slightly faster (4- to 5-fold) k_{obs} for this nucleotidyl step compared with the WT enzyme (Table 1; Fig. S4). The molecular basis for this observation is not known, but again supports the model of an active site that utilizes distinct active site features for the addition of incoming nucleotides depending on the type of base-paired interaction they make with the substrate tRNA.

Discussion

The interaction of Thg1 enzymes with the tRNA^{His} anticodon is a critical feature for selective tRNA recognition that is well-supported by both biochemical and structural data (23, 28). Nonetheless, the mechanism by which this interaction enables catalysis to occur at the 5′-end of tRNA, ~70 Å away from the anticodon, has remained largely a mystery. Here we carried out a detailed biochemical characterization of the catalytic role of two key tRNA-interacting residues in the context of human Thg1. Our data reveal dual functions for the conserved His-152 and Lys-187 residues in both the tRNA-anticodon interaction and in bp recognition during catalysis. This previously unknown catalytic role for the His-152 and Lys-187 side chains is most significantly observed on the 5′-end activation step for non-WC G_{-1} addition to tRNA^{His}, which is the essential physiological function of this enzyme in the majority of eukaryotic systems.

In the CaThg1-tRNA complex structure, a network of highly conserved residues, including the analogous residues to His-152 and Lys-187, are observed either interacting directly with or nearby the anticodon of the tRNA (23). Nonetheless, the relatively unchanged tRNA^{His} anticodon footprint with either of the variant enzymes suggests that the overall interaction with the anticodon loop is sustained in H152A and K187A variants that were previously believed to be entirely catalytically defective. The protections observed across the whole anticodon loop with hThg1 suggest that the interaction with this part of the tRNA is multifaceted. Therefore it may not be a surprise that any single mutation of these residues fails to abolish all interactions with the anticodon loop. Instead, the biological fidelity of Thg1 is apparently ensured through the combined effects of the interactions with a network of residues.

The 4:2 (Thg1:tRNA) stoichiometry revealed by the *C. albicans* tRNA-bound structure suggested the possibility of non-identical functions for individual monomeric subunits in the context of the tetrameric enzyme (23) (Fig. 1*B*). This study fur-

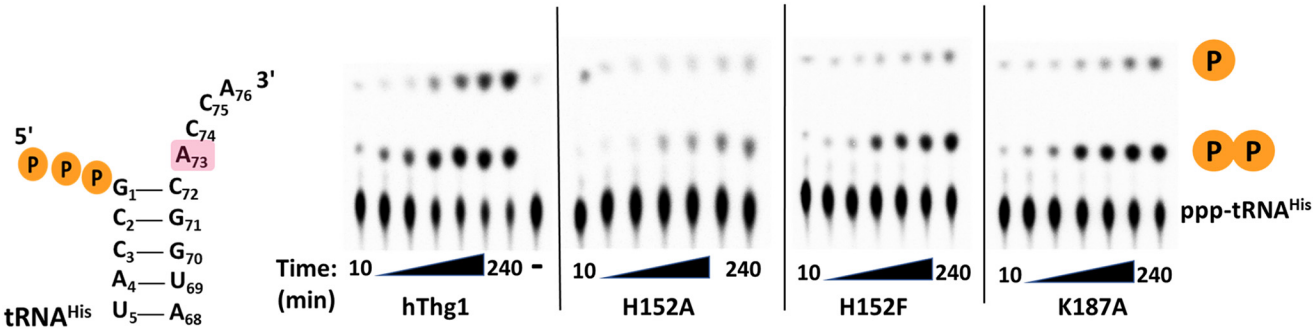

Figure 6. Thg1 variants perform non-WC nucleotidyl transfer on pre-activated tRNA substrate p*pptRNA^{His}. Nucleotidyl transfer experiments were performed under single turnover conditions of excess enzyme (15 μM), limiting amounts of 5′-end–labeled p*pptRNA substrate with an A_{73} discriminator and saturating concentration (1 mM) GTP. Reaction progress was analyzed over a 4-h time course (10, 20, 30, 90, 120, 180, and 240 min). Addition of the unlabeled GTP nucleotide to produce the G_{-1}:A_{73} bp results in the release of the labeled pyrophosphate from the tRNA substrate, which is visualized by TLC (some of the PPi can be further hydrolyzed to P_i during the long time course of the assay). The diagram to the *left* shows the aminoacyl-acceptor stem of the labeled tRNA^{His} substrate (the rest of the tRNA is omitted for clarity), with the labeled 5′ triphosphate moiety indicated in *orange*.

ther supports this scenario, providing the first examples of Thg1 residues that appear to have distinct molecular functions in the context of different Thg1 monomers. Although in the CaThg1-tRNA co-crystal structure, His-152 (His-154 in CaThg1) is located on α helix 5, which appears in close proximity to the tRNA 5′-end, the molecular nature of its catalytic function could not have been interpreted from the structure because of lack of electron density at the apparent site of G_{-1} addition. Here, however, kinetic studies imply a specific and unexpected role for His-152 and Lys-187 in the activation step for non-WC G_{-1} addition to tRNA^{His} (Figs. 4–6; Table 1) (19, 22, 23, 28). Although the molecular interactions that enable His-152 and Lys-187 to participate in this specific reaction cannot be discerned by available structural models, these residues are located in close proximity to known adenylylation residues Lys-44 and Asn-161, consistent with this role (Fig. 1*B*) (19, 23).

Interestingly, the catalytic role for His-152 appears to depend substantially on the aromatic nature of this residue, as judged from the recovery of activity with H152F but not Gln or Lys variants (Figs. 4–6). These biochemical data could be explained by a stabilizing interaction of His-152 with the incoming non-WC base-paired GTP nucleotide itself, which, interestingly, is analogous to the stacking interactions between the residue and G-nucleotides in the anticodon loop (23). The selective nature of the requirement for His-152/Lys-187 for the non-WC base-paired interaction could be explained by slightly different conformations of the active site when the incoming GTP forms a WC bp with the C_{73} nucleotide on this tRNA^{His} variant. If the WC bp is formed, apparently the optimal positioning of GTP for subsequent nucleotidyl transfer is achieved even in the absence of His-152 and Lys-187, and the reaction can proceed. The more significant kinetic effect on the activation step, which occurs prior to use of the incoming GTP (Fig. 1*A*), also suggests a picture of a preformed active site with both nucleotides (ATP for activation and GTP for nucleotidyl transfer) bound simultaneously.

This work provides further insight into two apparently distinct components of the active site that are involved in discriminating WC *versus* non-WC bp (17, 29). Other members of the Thg1 superfamily known as Thg1-like proteins (TLPs), which are found in all three domains of life, are strictly WC-dependent 3′ to 5′ polymerases that do not catalyze efficient non-WC G_{-1} addition (21, 29). Moreover, TLPs are not generally tRNA^{His}-selective enzymes that depend on the presence of the GUG anticodon (30–32). Therefore, it is intriguing that His-152 and Lys-187 are absolutely conserved residues in eukaryotic Thg1 enzymes but do not have obvious counterparts in TLPs. This suggests an evolutionary scenario where both WC-dependent and non-tRNA^{His}-specific activities of the ancestral 3′ to 5′ polymerases could have been simultaneously adapted in the earliest eukaryotic ancestor by the acquisition of a relatively limited number of amino acid changes. In this scenario, the emergence of dual function residues such as His-152 and Lys-187 would enable a single alteration to affect both catalytic activity and tRNA specificity of the enzyme.

Experimental procedures

Site-directed mutagenesis

Mutagenesis was performed using Phusion polymerase (Thermo Fisher) according to the manufacturer's instructions. Reactions contained 50 ng of template DNA encoding hThg1-His_6 and 0.5 μM for each primer (T_m < 80 °C, 36–49 nucleotides in length) (16). Following 25 rounds of temperature cycling, DNA was ligated, digested with DpnI (New England Biolabs), and transformed into *Escherichia coli* XLI-Blue cells. Plasmids from transformed colonies were isolated and sequenced to confirm mutation.

Human Thg1 expression and protein purification

Overexpression and purification by immobilized metal-ion affinity chromatography of C-terminal His_6-tagged human Thg1 variants was performed as described previously (16). Purified variant and WT Thg1 proteins were dialyzed into 50% glycerol buffer for storage at −20 °C. Purity of hThg1 proteins was qualitatively assessed by SDS-PAGE and protein concentrations were determined using the Bradford reagent (Bio-Rad).

In vitro transcription of tRNA substrates

Run-off transcription and labeling of tRNA^{His} containing either A_{73} or C_{73} discriminator nucleotide was performed as described previously (16). Briefly, *in vitro* transcripts were gel purified, extracted with phenol:chloroform, and precipitated with ethanol for storage at −20 °C in TE buffer, pH 7.5. To

generate 5′-^{32}P monophosphorylated tRNA (p*tRNA^{His}) for phosphatase protection assays, transcribed tRNA was treated with phosphatase (New England Biolabs) followed by T4 polynucleotide kinase in the presence of [γ-^{32}P]ATP (Perkin Elmer, 6000 Ci/mmol). Labeled 5′ triphosphorylated tRNA (p*pptRNA^{His}) used in nucleotidyl transfer experiments was transcribed in the presence of [γ-^{32}P]GTP (Perkin Elmer, 6000 Ci/mmol). Uniformly labeled tRNA^{His} used in filter binding experiments was *in vitro* transcribed in the presence of [α-^{32}P]GTP (Perkin Elmer, 3000 Ci/mmol). All labeled tRNAs were gel-purified and stored at −20 °C.

Chemical footprinting and primer extension

Chemical footprinting with CMCT was performed using unlabeled *in vitro* transcribed tRNA^{His}. Modification by CMCT was performed according to Ref. 33. Reactions contained 50 nM tRNA^{His} and 0, 1, or 5 μM hThg1 in Buffer B (10 mM potassium borate, pH 7.9, 100 mM KCl, 5 mM $MgCl_2$). Protein and tRNA were allowed to bind at room temperature for ∼1 h prior to chemical treatment. After binding, 5 μl of 25 mg/ml CMCT was added and reactions were placed at 4 °C for 2 h. Following incubation, reactions were quenched with 200 μl of Buffer B containing 20 μg of yeast carrier RNA and precipitated with 1/10 volume of 3 M sodium acetate, pH 5.3, and 2.5 volumes of 100% ethanol. Samples were precipitated again, resuspended in 4 μl of water, and stored at −20 °C. Reverse transcription primer (5′-TGGTGCCATCTCCTAG) for *S. cerevisiae* tRNA^{His} was 5′-end labeled in a kinase reaction with T4 PNK and [γ-^{32}P]ATP (6000 Ci/mmol, Perkin Elmer). Labeled primer (1 pmol) and CMCT treated/untreated RNA (2 pmol) were denatured at 95 °C for 5 min, then slowly cooled to room temperature to anneal. After annealing, 0.2 mM dNTPs, 5× reaction buffer, and reverse transcriptase (USB/Promega) was added to initiate reactions. Extension was performed for 5 min at 25 °C, followed by 37 °C for 1–2 h. An equal amount of 2× RNA loading dye (formamide, 0.5 M EDTA, pH 8, 10% bromphenol blue, and 10% xylene cyanol) was added to all samples, which were then resolved on a 10% polyacrylamide/8 M urea gel. Dried gels were visualized using GE Typhoon Trio Imager Scanner (GE Healthcare Life Sciences) and quantified by ImageQuant. To measure normalized CMCT reactivity, primer stop intensity at each position within tRNA treated with CMCT and in the presence and absence of each hThg1 variant was divided by the sum of that intensity and the intensity of fully extended RNA.

Filter-binding assay

Double-filter binding assays were performed as described in (18) with uniformly labeled tRNA^{His}. Briefly, varied concentrations of human Thg1 WT and variants (0.05–10 μM) were incubated with limiting amounts of tRNA and bound *versus* free RNA were separated by filtration through nitrocellulose and Hybond filters, respectively. The fraction of enzyme-bound tRNA was plotted as a function of enzyme concentration and fit to a binding isotherm to yield the apparent $K_{D,tRNAHis}$ (Fig. S2).

Thg1 activity assays with 5′-monophosphorylated tRNA^{His}

Phosphatase protection assays were performed as described previously (28). In brief, limiting concentrations of 5′ p*-tRNA^{His} were incubated with 5-fold dilutions WT and variant hThg1 (from 36 μM to 290 nM) in the presence of 1 mM each ATP and GTP at room temperature for 1–2 h, as indicated in each figure. Reactions testing for G_{-1} addition were treated with RNase A, whereas U_{-1} addition reactions were treated with RNase T1. Nuclease digested reactions were then treated with phosphatase (Invitrogen) producing the indicated oligonucleotide fragments corresponding to nucleotide addition products, or $^{32}P_i$ from unreacted substrate. A nonenzyme-catalyzed labeled species (*) is observed in these reactions as a consequence of the labeling process and has been indicated on all assay images. All reaction products are resolved by silica TLC using 1-propanol-NH_4OH-H_2O (55:35:10, v/v/v) solvent system.

To compare specific activity of each variant enzyme to WT, total percent product formation was quantified at each enzyme concentration, and 1 unit of total activity was set to reflect 30% product formation during the 2-h reaction. The concentration of enzyme required to catalyze 1 unit of activity was calculated and reported as the fraction of WT specific activity for each active enzyme.

Thg1 activity assay with 5′ triphosphorylated tRNA^{His}

Nucleotidyl transfer assays were executed as described previously (19). In brief, triphosphorylated p*pptRNA^{His} was incubated in the presence of excess (15 μM) hThg1 WT and variant enzymes at room temperature. At various time points (10–240 min), 2-μl aliquots were taken from the reaction and quenched with 0.25 M EDTA and 5 mg/ml RNase A (Ambion) then incubated at 50 °C for 10 min. Next, RNase-treated samples were treated with an equal volume of 10% trichloroacetic acid (TCA), incubated on ice for 5 min, and centrifuged for 5 min to pellet precipitated protein and improve clarity of TLC resolution. The supernatant after TCA precipitation was resolved on PEI cellulose TLC plates (EMD Millipore) in a 0.5 M KPO_4^-:CH_2OH (80:20, v/v) solvent system. All experiments were imaged using GE Typhoon Trio Imager Scanner and quantified using ImageQuant.

Observed rates (k_{obs}) were obtained by fitting the data to a single exponential equation (Eq. 1), where P_t is total product conversion at a time point, ΔP is the maximum percent product formed over the time course, and t is time.

$$P_t = \Delta P(1 - \exp(-k_{obs} * t) \quad \text{(Eq. 1)}$$

Rates for slow hThg1 variants that were not able to achieve maximal product formation during the time of the assays were determined using the method of initial rates (Eq. 2) where v_0, the slope obtained from percent product plotted against time is divided by the maximum percent of product produced, ΔP.

$$k_{obs} = v_0/\Delta P \quad \text{(Eq. 2)}$$

Author contributions—A. O. M., B. A. S., and J. E. J. conceptualization; A. O. M., B. A. S., and J. E. J. data curation; A. O. M., B. A. S., and J. E. J. formal analysis; A. O. M. and J. E. J. supervision; A. O. M. and J. E. J. funding acquisition; A. O. M., B. A. S., and J. E. J. investigation; A. O. M. and B. A. S. writing-original draft; A. O. M., B. A. S., and J. E. J. writing-review and editing.

Acknowledgment—Research reported in this publication was supported by the Office of the Director, National Institutes of Health under Award Number S10OD023582.

References

1. Phizicky, E. M., and Hopper, A. K. (2010) tRNA biology charges to the front. *Genes Dev.* **24,** 1832–1860 CrossRef Medline
2. Himeno, H., Hasegawa, T., Ueda, T., Watanabe, K., Miura, K., and Shimizu, M. (1989) Role of the extra G-C pair at the end of the acceptor stem of tRNA(His) in aminoacylation. *Nucleic Acids Res.* **17,** 7855–7863 CrossRef Medline
3. Rudinger, J., Florentz, C., and Giegé, R. (1994) Histidylation by yeast HisRS of tRNA or tRNA-like structure relies on residues −1 and 73 but is dependent on the RNA context. *Nucleic Acids Res.* **22,** 5031–5037 CrossRef Medline
4. Nameki, N., Asahara, H., Shimizu, M., Okada, N., and Himeno, H. (1995) Identity elements of *Saccharomyces cerevisiae* tRNA(His). *Nucleic Acids Res.* **23,** 389–394 CrossRef Medline
5. Rudinger, J., Felden, B., Florentz, C., and Giegé, R. (1997) Strategy for RNA recognition by yeast histidyl-tRNA synthetase. *Bioorg. Med. Chem.* **5,** 1001–1009 CrossRef Medline
6. Ardell, D. H., and Andersson, S. G. E. (2006) TFAM detects co-evolution of tRNA identity rules with lateral transfer of histidyl-tRNA synthetase. *Nucleic Acids Res.* **34,** 893–904 CrossRef Medline
7. Wang, C., Sobral, B. W., and Williams, K. P. (2007) Loss of a universal tRNA feature. *J. Bacteriol.* **189,** 1954–1962 CrossRef Medline
8. Rao, B. S., Mohammad, F., Gray, M. W., and Jackman, J. E. (2013) Absence of a universal element for $tRNA^{His}$ identity in *Acanthamoeba castellanii*. *Nucleic Acids Res.* **41,** 1885–1894 CrossRef Medline
9. Rao, B. S., and Jackman, J. E. (2015) Life without post-transcriptional addition of G_{-1}: Two alternatives for $tRNA^{His}$ identity in Eukarya. *RNA* **2,** 243–253 CrossRef Medline
10. Cooley, L., Appel, B., and Söll, D. (1982) Post-transcriptional nucleotide addition is responsible for the formation of the 5′ terminus of histidine tRNA. *Proc. Natl. Acad. Sci. U.S.A.* **79,** 6475–6479 CrossRef Medline
11. Burkard, U., and Söll, D. (1988) The 5′-terminal guanylate of chloroplast histidine tRNA is encoded in its gene. *J. Biol. Chem.* **263,** 9578–9581 Medline
12. Burkard, U., Willis, I., and Söll, D. (1988) Processing of histidine RNA precursors. *J. Biol. Chem.* **263,** 2447–2451 Medline
13. L'Abbé, D., Lang, B. F., Desjardins, P., and Morais, R. (1990) Histidine tRNA from chicken mitochondria has an uncoded 5′-terminal guanylate residue. *J. Biol. Chem.* **265,** 2988–2992 Medline
14. Placido, A., Sieber, F., Gobert, A., Gallerani, R., Giegé, P., and Maréchal-Drouard, L. (2010) Plant mitochondria use two pathways for the biogenesis of $tRNA^{His}$. *Nucleic Acids Res.* **38,** 7711–7717 CrossRef Medline
15. Orellana, O., Cooley, L., and Soll, D. (1986) The additional guanylate at the 5′ terminus of *Escherichia coli* $tRNA^{His}$ is the result of unusual processing by RNase P. *Mol. Cell. Biol.* **2,** 525–529 Medline
16. Gu, W., Jackman, J. E., Lohan, A. J., Gray, M. W., and Phizicky, E. M. (2003) $tRNA^{His}$ maturation: An essential yeast protein catalyzes addition of a guanine nucleotide to the 5′ end of $tRNA^{His}$. *Genes Dev.* **17,** 2889–2901 CrossRef Medline
17. Jackman, J. E., and Phizicky, E. M. (2006) $tRNA^{His}$ guanylyltransferase catalyzes a 3′-5′ polymerization reaction that is distinct from G_{-1} addition. *Proc. Natl. Acad. Sci. U.S.A.* **103,** 8640–8645 CrossRef Medline
18. Hyde, S. J., Eckenroth, B. E., Smith, B. A., Eberley, W. A., Heintz, N. H., Jackman, J. E., and Doublié, S. (2010) $tRNA^{His}$ guanylyltransferase (THG1), a unique 3′-5′ nucleotidyl transferase, shares unexpected structural homology with canonical 5′-3′ DNA polymerases. *Proc. Natl. Acad. Sci. U.S.A.* **107,** 20305–20310 CrossRef Medline
19. Smith, B. A., and Jackman, J. E. (2012) Kinetic analysis of 3′-5′ nucleotide addition catalyzed by eukaryotic $tRNA^{His}$ guanylyltransferase. *Biochemistry* **51,** 453–465 CrossRef Medline
20. Jahn, D., and Pande, S. (1991) Histidine tRNA guanylyltransferase from *Saccharomyces cerevisiae*. II. Catalytic mechanism. *J. Biol. Chem.* **266,** 22832–22836 Medline
21. Jackman, J. E., Gott, J. M., and Gray, M. W. (2012) Doing it in reverse: 3′-to-5′ polymerization by the Thg1 superfamily. *RNA* **18,** 886–899 CrossRef Medline
22. Jackman, J. E., and Phizicky, E. M. (2008) Identification of critical residues for G_{-1} addition and substrate recognition by $tRNA^{His}$ guanylyltransferase. *Biochemistry* **47,** 4817–4825 CrossRef Medline
23. Nakamura, A., Nemoto, T., Heinemann, I. U., Yamashita, K., Sonoda, T., Komoda, K., Tanaka, I., Söll, D., and Yao, M. (2013) Structural basis of reverse nucleotide polymerization. *Proc. Natl. Acad. Sci.* **110,** 20970–20975 CrossRef Medline
24. Hyde, S. J., Rao, B. S., Eckenroth, B. E., Jackman, J. E., and Doublié, S. (2013) Structural studies of a bacterial $tRNA^{His}$ guanylyltransferase (Thg1)-like protein with nucleotide in the activation and nucleotidyl transfer sites. *PLoS One* **8,** e67465 CrossRef Medline
25. Lee, K., Lee, E. H., Son, J., and Hwang, K. Y. (2017) Crystal structure of $tRNA^{His}$ guanylyltransferase from *Saccharomyces cerevisiae*. *Biochem. Biophys. Res. Commun.* **490,** 400–405 CrossRef Medline
26. Desai, R., Kim, K., Büchsenschütz, H. C., Chen, A. W., Bi, Y., Mann, M. R., Turk, M. A., Chung, C. Z., and Heinemann, I. U. (2018) Minimal requirements for reverse polymerization and tRNA repair by $tRNA^{His}$ guanylyltransferase. *RNA Biol.* **15,** 614–622 CrossRef Medline
27. Kimura, S., Suzuki, T., Chen, M., Kato, K., Yu, J., Nakamura, A., Tanaka, I., and Yao, M. (2016) Template-dependent nucleotide addition in the reverse (3′-5′) direction by Thg1-like protein. *Sci. Adv.* **2,** e1501397 CrossRef Medline
28. Jackman, J. E., and Phizicky, E. M. (2006) $tRNA^{His}$ guanylyltransferase adds G_{-1} to the 5′ end of $tRNA^{His}$ by recognition of the anticodon, one of several features unexpectedly shared with tRNA synthetases. *RNA* **12,** 1007–1014 CrossRef Medline
29. Abad, M. G., Rao, B. S., and Jackman, J. E. (2010) Template-dependent 3′-5′ nucleotide addition is a shared feature of $tRNA^{His}$ guanylyltransferase enzymes from multiple domains of life. *Proc. Natl. Acad. Sci.* **107,** 674–679 CrossRef Medline
30. Abad, M. G., Long, Y., Willcox, A., Gott, J. M., Gray, M. W., and Jackman, J. E. (2011) A role for tRNA(His) guanylyltransferase (Thg1)-like proteins from *Dictyostelium discoideum* in mitochondrial 5′-tRNA editing. *RNA* **17,** 613–623 CrossRef Medline
31. Long, Y., Abad, M. G., Olson, E. D., Carrillo, E. Y., and Jackman, J. E. (2016) Identification of distinct biological functions for four 3′-5′ RNA polymerases. *Nucleic Acids Res.* **44,** 8395–8406 CrossRef Medline
32. Rao, B. S., Maris, E. L., and Jackman, J. E. (2011) tRNA 5′-end repair activities of $tRNA^{His}$ guanylyltransferase (Thg1)-like proteins from Bacteria and Archaea. *Nucleic Acids Res.* **39,** 1833–1842 CrossRef Medline
33. Rio, D. C, Ares, M., Jr., Hannon, G. J., and Nilsen, T. W. (2011) Mapping sites of RNA-protein interactions using chemical methods. in *RNA: a Laboratory Manual*, pp. 276–283 Cold Spring Harbour Laboratory Press, New York